# Guide to video recording of structure dynamics and dynamic processes of proteins by high-speed atomic force microscopy

Takayuki Uchihashi[1,2], Noriyuki Kodera[2] & Toshio Ando[1,2]

[1]Department of Physics, Kanazawa University, Kanazawa, Japan. [2]Bio-AFM Frontier Research Center, Kanazawa University, Kanazawa, Japan. Correspondence should be addressed to T.A. (tando@staff.kanazawa-u.ac.jp).

Published online 24 May 2012; doi:10.1038/nprot.2012.047

**High-speed atomic force microscopy (HS-AFM) allows direct visualization of dynamic structural changes and processes of functioning biological molecules in physiological solutions, at subsecond to sub-100-ms temporal and submolecular spatial resolution. Unlike fluorescence microscopy, wherein the subset of molecular events that you see is dependent on the site where the probe is placed, dynamic molecular events unselectively appear in detail in an AFM movie, facilitating our understanding of how biological molecules function. Here we present protocols for HS-AFM imaging of proteins in action, including preparation of cantilever tips, step-by-step procedures for HS-AFM imaging, and recycling of cantilevers and sample stages, together with precautions and troubleshooting advice for successful imaging. The protocols are adaptable in general for imaging many proteins and protein–nucleic acid complexes, and examples are described for looking at walking myosin, ATP-hydrolyzing rotorless $F_1$-ATPase and cellulose-hydrolyzing cellulase. The entire protocol takes 10–15 h, depending mainly on the substrate surface to be used.**



## INTRODUCTION

Proteins perform their functions through their dynamic structural changes and dynamic interactions with other molecules. Even cellular structures made of protein are highly dynamic. Therefore, in the quest for better understanding of biological phenomena, acquiring details of structure dynamics and dynamic interplay between subunits within a protein and between proteins is essential. Although the structure of proteins has been studied by X-ray crystallography, electron microscopy, NMR and atomic force microscopy (AFM), structures obtained are static snapshots. The dynamic behavior of proteins has been studied by single-molecule fluorescence microscopy and optical trap nanometry, but protein molecules themselves are invisible in the observations. To understand how proteins perform their functions, inferences have to be made from collected data with substantial resolution gaps. Directly visualizing functioning protein molecules at high spatiotemporal resolution has therefore been an important goal for structural biology and biophysics.

AFM is now routinely used to directly acquire high-resolution images of biological samples under physiological conditions, without sample staining[1]. To form an image, AFM acquires the sample height information over many points on the sample. During the acquisition at each point, a sharp tip attached to the free end of a cantilever is brought into contact with the sample. The mechanical response of the cantilever upon this contact (change in, e.g., deflection, oscillation amplitude, oscillation phase or resonant frequency, depending on the AFM operation mode to be used) is measured and then the sample stage is moved in the *z*-direction to recover the mechanical state of the cantilever back to a given state (i.e., set point) through feedback control. Without this feedback control, the force exerting from the cantilever tip to the sample cannot be kept constant, resulting in serious damage or disruption of the sample. The closed feedback loop, in which various devices are contained, requires an amount of time for this recovery that depends mainly on the slow response of the mechanical devices (i.e., cantilever and *z*-scanner). This series of operations is repeated many times for different points on the sample during lateral scanning of the sample stage, which means that it takes a relatively long time (at least 30 s) to get an image.

Over the past 15 years, various efforts were carried out to increase the imaging rate of AFM[2–13], and HS-AFM has now materialized[14,15] (see recent reviews[16–18]). HS-AFM uses a small cantilever with a high-resonant frequency (the first resonant frequency $f_c$ = 0.6 − 1.2 MHz in water) and a small spring constant ($k_c$ = 0.1–0.2 N m$^{-1}$). The HS-AFM instrument comprises a fast scanner, a feedback controller, fast electronics and an optical beam deflection (OBD) detector for detecting deflection of this small cantilever (**Fig. 1**). The system is operated in the tapping mode; a cantilever is oscillated at $f_c$ in the *z*-direction so that its tip is brought intermittently into contact with the sample. It allows imaging at a rate of 5–20 frames per second (fps) without disturbing the function of fragile proteins and delicate protein-protein and DNA-protein interactions.

This high-speed and minimally invasive performance opens up a new opportunity to directly visualize dynamic events of proteins[19–27], DNA-protein complexes[28–30] and other molecular systems[31–33]. In this protocol, we describe various preparations and procedures to be done before the actual imaging experiments, how to use the HS-AFM instrument to image dynamic events of proteins and cleanup steps for the next imaging experiments (**Fig. 2**). As designing substrate surfaces is particularly important for successful imaging, we provide, for example, a procedure for preparing mica-SLBs (supported lipid bilayers; Steps 15–18). Mica-SLBs containing biotin- or Ni-NTA–conjugated lipids are useful for selective immobilization of proteins with either biotin or His-tag, respectively[34,35]. Mica-SLBs can also be used for electrostatic immobilization of proteins under a controlled surface charge density[19,34,35]. We describe three options for sample deposition: direct sample deposition onto a bare surface of mica or HOPG

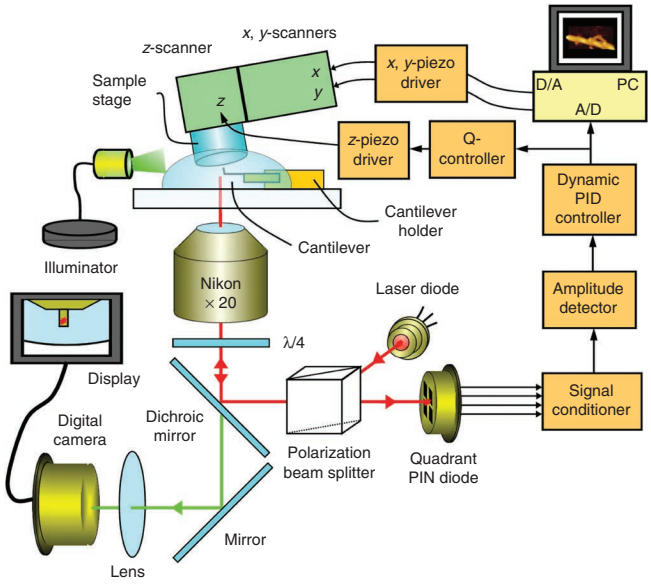


**Figure 1** | Schematic of the HS-AFM system.

(highly ordered pyrolytic graphite; the example described is the one used for looking at cellulase-hydrolyzing cellulose[23]); covalent immobilization of proteins onto a mica surface with glutaraldehyde (the example described is the one used for looking at rotary catalysis of rotorless $F_1$-ATPase[22]); and sample deposition onto mica-SLBs (the example described is the one we used for looking at walking myosin[19]).

We also provide videos to show procedures for imaging. We have used this protocol in our previous studies on myosin V[19], bacteriorhodopsin (bR)[20,21,24], rotorless $F_1$-ATPase[22] and cellulases[23], and example results can be found in the ANTICIPATED RESULTS section. The protocol can be adapted to many other biomolecular systems, mainly by optimizing the substrate surface onto which the molecules are placed. More details on the preparation of substrate surfaces and considerations for their choice are given elsewhere[34–36].

### Sources of supply of HS-AFM equipment and cantilevers

Currently, only a small number of laboratories are using HS-AFM because the availability of the equipment has been limited until recently. However, HS-AFM equipment, which is a copy of our homemade apparatus, is now available from a manufacturer, RIBM (Tsukuba, Japan). This system is the fastest one, and other nominal HS-AFM systems from different manufacturers are at least ten times slower. Therefore, some aspects of the present protocol are specific to the HS-AFM equipment manufactured by RIBM. Small cantilevers made of silicon nitride (9–10 μm long, 2 μm wide and 130 nm thick; BL-AC10DS, Olympus, Tokyo) with $f_c$ = 1.5 MHz in air and 0.6 MHz in water, $k_c$ = 0.1 N m$^{-1}$, and a quality factor $Q$ ~2 in water (**Fig. 3**) are available from Olympus, Atomic Force F&E, Asylum Research and Bruker. Smaller cantilevers (BL-AC7DS-KU2; 6–7 μm long, 2 μm wide and 90 nm thick) with $f_c$ = 3.5 MHz in air and 1.2 MHz in water, $k_c$ = 0.2 N m$^{-1}$, and $Q$ ~2 in water can be custom-made by Olympus. We have been mostly using the latter type. These cantilevers have bird beak–like tips, but electron-beam deposited (EBD) sharper tips are available as option. Moreover, prototypical small cantilevers ($k_c$ = 0.15 N m$^{-1}$ and $f_c$ = 1.2 MHz in air) are also available from NanoWorld.

### Overview of HS-AFM system

The HS-AFM system includes an original inverted optical microscope (**Fig. 1**). An objective lens with a long working distance of 24 mm (CFI L Plan EPI SLWD ×20, Nikon, Tokyo) that is used for the optical microscope is a part of the OBD detector, and is also used for viewing the cantilever and sample stage under the optical microscope via a digital camera or a CCD camera[4,15]. A 0.5-mm thick glass slide, to which a cantilever holder and a liquid cell are attached, is placed on the optical microscope stage. A cantilever chip is held in the holder so that its tip points upward (opposite to the way in conventional AFM)[4,15]. A sample stage, attached to the $z$-scanner and facing downward, is placed over the cantilever. An incident laser beam passing through the objective lens is focused onto the small cantilever, and the light reflected back from the cantilever is collected and collimated by the same objective lens and guided to a quadrant-cell Si PIN photodiode[4,15]. The incident and reflected laser beams are separated using a quarter-wavelength (λ/4) plate and a polarization beam splitter[4,15].

Three types of scanners with different maximum scan ranges are available. Type 1: $x$ = 1 μm, $y$ = 4 μm, $z$ = 1 μm; Type 2: $x$ = 5 μm, $y$ = 5 μm, $z$ = 2 μm; and Type 3: $x$ = 40 μm, $y$ = 40 μm, $z$ = 6 μm. Type 1 is used for dynamic imaging of isolated proteins, whereas the latter two types are used for dynamic imaging of larger objects such as bacteria and eukaryotic cells. Q-control circuits with mock $z$-scanners (LRC circuits) are implemented to their $z$-scanners to damp mechanical vibrations[6]. In these scanners, the $x$-scan is made though inverse transfer function compensation to damp unwanted vibrations[15]. The feedback controller (termed 'dynamic proportional-integral-derivative (PID) controller') contains a circuit for suppressing or eliminating a tip 'parachuting' effect[8]. In this context, parachuting means that the tip completely detaches from the sample surface at inclined regions of the sample, and time elapses until it lands on the surface again. In conventional PID controllers, parachuting often occurs when the cantilever amplitude set point is set very close to the free oscillation amplitude so that the tip lightly taps the sample surface[8,15].

### Spatial and time resolutions

In comparison with conventional large cantilevers, the small cantilevers afford ~10–20 times higher sensitivity to the detection of cantilever oscillation amplitude by the OBD detector and the amplitude detector. Even though the bandwidth for detection at every oscillation cycle (~0.83 μs period) is high, good (~0.1 nm) precision (hence, spatial resolution in the $z$-dimension) is achieved[15]. The spatial resolution in the $x$–$y$ dimensions depends on the radius of the tip apex. However, it is limited to 1–2 nm even when a tip with an apex radius of ~0.5 nm is used[22,37].

The time resolution $T$ depends on the feedback bandwidth $f_B$, which is a function not only of the speed performance of devices contained in the feedback loop but also of the ratio of the cantilever oscillation amplitude $A_0$ to the maximum sample height $h_0$ (the amplitude set point generally affects $f_B$, but in practice this is not seen because the dynamic PID controller is used)[8,15]. However, for relatively small protein molecules, $f_B$ can be approximately considered to be ~110 kHz. The time resolution $T$ is also a function of the scan range in the $x$-direction $W$, the number of scan lines $N$,

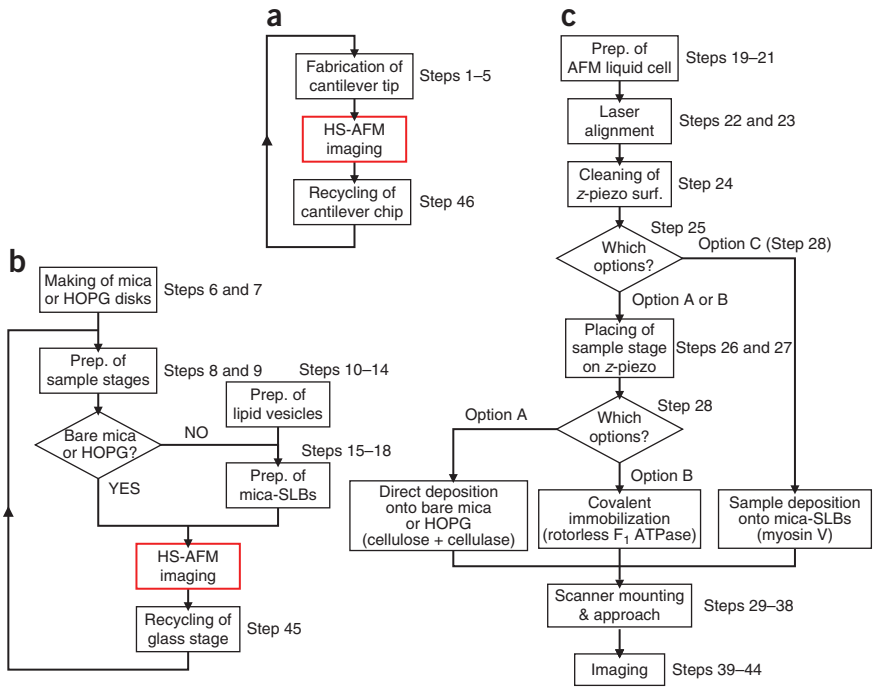


**Figure 2** | Flowcharts showing overview of procedures before and during HS-AFM imaging and cleanup steps for the next imaging experiments. (**a**) Works for cantilevers. (**b**) Works for substrate surface preparation and sample deposition. (**c**) Procedures of high-speed AFM imaging.

the smallest sample surface corrugation to be observed $\lambda$ and the sample fragility. The overall relationship can be expressed as

$$T = \pi WN/(2\lambda f_B \theta_m), \quad (1)$$

where $\theta_m$ represents an sample fragility-dependent allowable maximum phase delay in the feedback control[15,18]. The meaning of the phase delay $\theta$ in the feedback control can be explained as follows; supposing that the sample surface has a sinusoidal shape with the periodicity $\lambda$ and the maximum height $h_0$ and that the sample stage is moved in the $x$-direction at velocity $V_s$, the sample height $h$ right under the cantilever tip changes with time $t$ as

$$h(t) = (h_0/2) \times \sin(2\pi ft), \quad (2)$$

where $f$ is the feedback frequency at which the $z$-scanner is moved and is given by $f = V_s/\lambda$. Because of feedback delay (delay time, $\tau_0$), the sample stage is moved in the $z$-direction as

$$Z(t) = -(h_0/2) \times \sin[2\pi f(t-\tau_0)]. \quad (3)$$

So, the phase delay $\theta$ is given by $\theta = 2\pi f\tau_0 = 2\pi V_s\tau_0/\lambda$.

### Tip force versus imaging rate

The sum of $h(t)$ and $Z(t)$ is the feedback error $E(t)$ and expressed as

$$E(t) = h_0 \times \sin(\theta/2) \times \cos(2\pi ft - \theta/2). \quad (4)$$

Therefore, because of the phase delay, the force given by $(k_c/Q) \times h_0 \times \sin(\theta/2)$ is excessively exerted at maximum from the tip to the sample, in addition to a constant force (~20–30 pN). For example, for biomolecules with $h_0$ ~5 nm, the force amounts to a maximum of ~100 pN when phase delay occurs by ~20–30°. However, note that the mechanical quantity that affects the sample (i.e., causes a momentum change) is not force itself but impulse (force × force acting time). The force acting time is very short (~100 ns or less) when a cantilever oscillating at 0.6–1.2 MHz is used. For relatively fragile protein molecules, $\theta_m \leq$~20°, whereas for relatively strong molecules $\theta_m$ can be extended to 45° or further. For example, under the imaging condition used for rotorless $F_1$-ATPase ($W$ = 80 nm, $N$ = 50 for a scan range of 40 nm in the $y$-direction, $\lambda$ = 2 nm, and $\theta_m$ ~ 20°), Equation (1) estimates that images can be captured at ~12.2 fps without damage to the sample. Consistent with this estimation, rotorless $F_1$-ATPase was successfully imaged at 12.5 fps with $A_0$ ~1 nm, without the function being disturbed[22]. Equation (1) provides a guideline for the allowable highest imaging rate under a given imaging condition. However, it should be determined by repeating test imaging on target biological samples, because the feedback phase delay cannot be measured during actual imaging. When the phase delay exceeds $\theta_m$, the sample is damaged. For example, when GroEL attached to a bare mica surface in the end-up orientation is imaged too fast, its top layer of the double ring is removed. As GroEL is commercially available and easily deposited on the surface of bare mica[3,38], it is a good test sample that one can use to check whether the HS-AFM setup itself works well and to examine the speed performance of other AFM systems.

### Experimental design and control experiment

The experimental design depends on the target sample and dynamic events to be visualized. For example, in the observation of myosin V walking along an actin filament[19], we first placed actin filaments and myosin V on the surface of bare mica under buffer solutions with various ionic strengths. Then, we chose an appropriate ionic

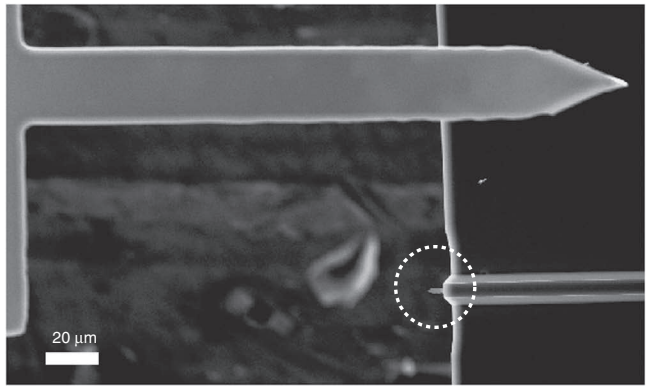


**Figure 3** | SEM micrograph of a conventional AFM cantilever (Olympus OMCL-AC240TS) and a small cantilever (Olympus BL-AC10DS; encircled).

strength, in which actin filaments stably attached to the surface while myosin V molecules were diffusing on the surface. Under this condition, we could observe myosin V molecules walking in a hand-over-hand manner, but its success rate was low; moreover, the walking velocity was much lower than that measured by fluorescence microscopy under the same buffer solution condition. We then chose electrically neutral mica-SLBs containing a biotin lipid. Partially biotinylated actin filaments were immobilized on the surface via streptavidin. Myosin V was never bound to the surface and only interacted with the immobilized actin filaments to move unidirectionally. However, most of the molecules were moving, orienting perpendicularly to the surface, so that we could not look at the characteristic sideways topography of the moving molecules. Next, we added a positively charged lipid in the bilayer in various densities. An appropriate density of the positively charged lipid was chosen so that we could observe the sideways topography of the molecules moving at velocity similar to that measured by fluorescence microscopy. However, the molecular process occurring during a step could not be resolved because it completes within a frame time (~143 ms). Finally, streptavidin molecules were further placed on the substrate surface as moderate obstacles to the advance. This final design allowed the visualization of detailed stepping processes.

It is important to check the possible effect of the tip-sample interaction on the visualized molecular events. When a time constant for an observed dynamic event is previously known, it should be compared with that obtained from the HS-AFM images. When it is unknown, the imaging rate should be changed in a possible range to examine whether the imaging rate (and hence the excessive force determined by the rate) affects the time constant, as has been done for the visualization of bR trimers that are binding to and dissociating from the edge region of two-dimensional crystal of bR in the purple membrane[24]. This check is particularly crucial when dynamic dissociation events of protein-protein or DNA-protein are imaged, because their dissociation is forced to occur by overly strong tip-sample interaction force.

One round of HS-AFM imaging of several molecules that appear in a few different scan areas generates many frames, so that we can thereby get statistically meaning results. As the same species of protein or DNA molecules have no individuality, quantitative analysis of a few molecules is sufficient as far as many frames have been captured for them. However, note that bacteria, mammalian cells and intracellular organelles are likely to have individuality within the same species, as has been indicated by a recent study of HS-AFM imaging of *E. coli* cells[39].



## MATERIALS

### REAGENTS

▲ **CRITICAL** All reagents should be of analytical grade.

- 1,2-Dipalmitoyl-*sn*-glycero-3-phosphocholine (DPPC; Avanti Polar Lipids)
- 1,2-Dipalmitoyl-3-trimethylammonium-propane (DPTAP; Avanti Polar Lipids)
- 1,2-Dipalmitoyl-*sn*-glycero-3-phosphoethanolamine-*N*-(cap biotinyl) (Biotin-cap-DPPE; Avanti Polar Lipids)
- Streptavidin (Wako)
- Chick brain myosin V-HMM[40,41]
- Rabbit skeletal actin[42]
- $\alpha(His_6$ at N terminus/C193S$)_3\beta(His_3$-Lys$_7$ at N terminus$)_3$ subcomplex of the $F_1$-ATPase from thermophilic *Bacillus sp.* PS3 expressed in *E. coli*[22]
- Crystalline cellulose from the cell wall of green alga *Cladophora sp.*[43]
- Cellulase (Cel7A) from *Tricoderma ressei*[44]
- Biotin-$(AC5)_2$ Sulfo-OSu (Dojindo)
- Phalloidin (Invitrogen)
- 3-Aminopropyl-triethoxysilane (Shin-Etsu Chemical) ! **CAUTION** It is harmful to skin. Rubber gloves and safety glasses should be used. Store in a light-resistant bottle whose cap is sealed with Parafilm.
- Glutaraldehyde (25% (wt/vol); Wako) ! **CAUTION** It is harmful to skin. Rubber gloves and safety glasses should be used. Store in a light-resistant bottle whose cap is sealed with Parafilm.
- Phenol (Nacalai Tesque) ! **CAUTION** It is harmful to the skin. Rubber gloves and safety glasses should be used.
- Epoxy adhesive (high-quick or Super X black; Cemedine)
- Colorless nail polish (available at supermarkets)
- Acetone (Nacalai Tesque)
- Water purified with Milli-Q (Millipore)
- Sodium acetate
- $MgCl_2$
- Tris-HCl
- KCl
- EGTA
- Imidazole
- DTT
- Chloroform
- Methanol
- HEPES
- NaOH
- $MgSO_4$

### EQUIPMENT

- Mica (natural Muscovite mica; The Nilaco Corporation)
- HOPG (ZYH grade; Bruker)
- Gel-Film (WF-55-X0-A; Gel-Pack)
- Flat plastic container with Gel-Film glued onto the inner plane. This is used for storing small cantilevers with sharpened EBD tips
- Auto-dry cabinet (Dry Keeper; Sanplatec) for storing scanners and cantilevers
- Syringe-driven filter (0.22 μm, Millex GV; Millipore)
- Precision wipes (Kimwipes; Kimberly-Clark)
- Wipes for optics (Super cloth SA-25; Asahi Kasei)
- Transparent container of cosmetic cream as a sealed container (volume, ~10 ml; available at supermarkets) to be used for mica-SLB preparation
- Glass rods as sample stages (custom-made, 1.5 or 2.0 mm in diameter and 2 mm in height; Japan Cell)
- Container made of aluminum with a lid having through-holes of 0.1 mm in diameter (custom-made; see **Fig. 4**). This container is used for fabricating EBD tips
- Cantilever holder for growing EBD tips (custom-made; see **Fig. 4**)
- Laboratory-built high-speed AFM (Nano Explore; recently commercialized by RIBM)
- Small cantilevers (BL-AC7DS-KU2; Olympus)
- Bath sonicator (40 W; Elmasonic One; Elma)
- Probe sonicator (10 W; UR-20P; Tomy Seiko)
- Stereoscopic microscope (L-50; Hozan)
- Rubber hand blower (Z-263; Hozan)
- Peristaltic pump (TP-10SA; As One Corporation)
- Field emission scanning electron microscope (FE-SEM; SUPRA40VP; Zeiss)
- Radiofrequency (RF) plasma etcher (PE-2000; South Bay Technology)
- Puncher set for preparing mica and HOPG disks (constructed using, e.g., Mini straight punch, punch guide bush and button die; Misumi Corporation)

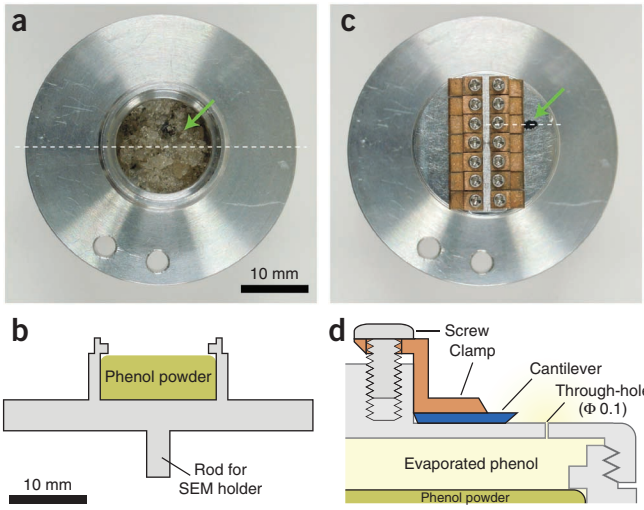


**Figure 4** | Pictures and schematics of a container for growing EBD tips with SEM. (**a**) Top view of the container without the lid. Phenol power therein is seen (arrow). (**b**) Cross-section of the container along the dotted line drawn in **a**. (**c**) Top view of the cantilever holder placed on the container lid. Fourteen cantilevers can be clamped to the holder with copper clamps. The arrow indicates a clamped cantilever. (**d**) Cross-section of the cantilever holder placed on the container along the dotted line drawn in **c**. The through-holes are positioned so that each through-hole is close to the distal end of each clamped cantilever.

### REAGENT SETUP

**Buffer solutions** Filter all buffer solutions using 0.22-µm syringe-driven filters and stock them in well-cleaned glass bottles. ▲ CRITICAL It is important to stock the buffer solutions in cleaned glass bottles (not in plastics bottles). Otherwise, many particles that may hamper the intended imaging will appear in AFM images.

**Imaging buffer for cellulose and cellulase (buffer A)** Imaging buffer is sodium acetate (20 mM, pH 5.0). It can be stored at 4 °C for a few months.

**Imaging buffer for rotorless $F_1$-ATPase (buffer B)** Combine 2 mM $MgCl_2$, 10 mM Tris-HCl (pH 8.0), and various concentrations of nucleotides. It can be stored at 4 °C for a few months.

**Imaging buffer for actomyosin V (buffer C)** Combine 25 mM KCl, 2 mM $MgCl_2$, 1 mM EGTA, 20 mM imidazole/HCl (pH 7.6), 5 mM DTT, and various concentrations of nucleotides. It can be stored at 4 °C for a few months.

**Nail polish** Dilute colorless nail polish three times with acetone. ▲ CRITICAL This dilution is very effective for quickly gluing a sample stage glass rod onto the *z*-piezo (*z*-scanner) and for fixing it firmly.

### EQUIPMENT SETUP

**High-speed AFM instrument** The imaging rate of HS-AFM is much higher than that of conventional slow AFM. Therefore, HS-AFM imaging is not hampered by slow mechanical and electrical drifts, meaning that we do not have to wait at all until the drifts cease. Moreover, effects on the image quality of varying imaging parameters, such as the amplitude set point and the PID controller gains, appear instantly on the acquired images. This excellent performance facilitates the tuning of imaging parameters for attaining high-quality images.

**Small cantilevers** As already mentioned, we use the small cantilevers custom-made by Olympus (BL-AC7DS-KU2). The apex of the beak-like tip of the cantilevers is not small enough (25–100 nm) to acquire high-resolution images. Therefore, we grow an EBD tip at the top end of the original beak-like tip using the FE-SEM. The EBD tip can be sharpened by argon or oxygen plasma etching. Note that the EBD tip can be completely removed by oxygen plasma etching over 1 d, so that we can reuse a small cantilever chip several times.



### PROCEDURE

▲ CRITICAL Note that stages of the procedure that need to be modified for different sample types (myosin V, rotorless $F_1$-ATPase and cellulose + cellulase) are indicated by the word "modify" in parenthesis.

**Fabrication of cantilever tips ● TIMING 3–5 h (depending on the number of cantilevers)**

**1|** Place a small amount of phenol powder (0.1–0.5 g) into the small container (volume, ~1 ml; **Fig. 4a**,**b**) with small through-holes (~0.1 mm diameter) in the lid[15].

**2|** Place small cantilevers into the cantilever holder (**Fig. 4c**,**d**). To reduce mechanical drift, the cantilevers should be tightly fixed in the holder using mechanical clamps. Do not use double-sided adhesive tape to fix cantilevers onto the container lid. Adjust the position of the holder relative to the lid so that each cantilever is positioned near a through-hole drilled in the lid. Note that it is not necessary to coat the small cantilevers with osmium to make them conductive if you use the low vacuum mode available in an SEM.

**3|** Place the container in the FE-SEM chamber and wait for 1–2 h until mechanical drift ceases.

**4|** Focus a spot-mode electron beam onto each original tip (**Fig. 5a**). It produces a stylus composed of amorphous carbon at a growth rate of ~17 nm $s^{-1}$ under low-vacuum conditions. The focused electron beam is usually irradiated onto the original tip for ~1 min, which results in growth of a ~1 µm long EBD tip (**Fig. 5b**). We can fabricate an EBD tip every 5 min. ▲ CRITICAL STEP Search for an appropriate SEM condition for growing sharp EBD tips. Typically, small working distance (3–4 mm), standard aperture size (for example, 30 µm), high acceleration voltage (higher than 20 kV), small spot size, well-turned focus and good stigma adjustment produce sharper EBD tips. Furthermore, the spot-mode electron beam should be applied at an angle relative to the original beak-tip so that in HS-AFM imaging the EBD tip touches the substrate surface perpendicularly (**Fig. 5b**). Thus, the cantilevers (hence, the container) should be set in the SEM chamber with a certain tilt angle (typically 10°).

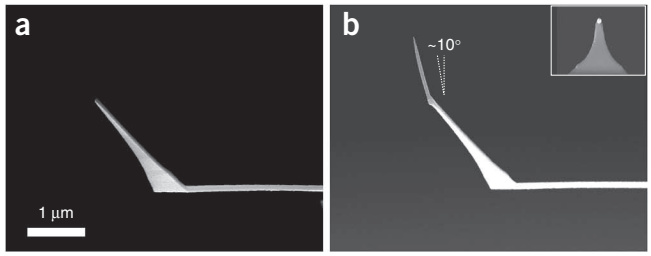


**Figure 5** | SEM photographs of small cantilevers with and without EBD tip. (**a**) An original beak-like tip. (**b**) Approximately 1-μm-long EBD tip grown on the original tip. The EBD tip makes an angle of ~10° relative to the normal line of the lever plane so that in HS-AFM imaging the tip taps the substrate surface perpendicularly. The inset shows a top view of the cantilever end with the EBD tip.

**5|** After fabricating EBD tips, remove the container from the SEM chamber while holding the cantilever holder. Attach the cantilevers to a glass slide using double-sided adhesive tape and put the glass slide into the RF-plasma etcher chamber. Apply argon or oxygen plasma etching to sharpen the EBD tips for ~8 min. Typical power of the RF plasma is about 18 W and the gas pressure is ~180 mTorr. It can reduce the apex radius from 15–25 to 4–5 nm. In the best case, it can be reduced to 0.5 nm, although the yield for tips of this radius is ~0.1 (refs. 20,22).

■ **PAUSE POINT** For convenience and time saving, fabricate many cantilever tips at once. After fabrication, put the small cantilevers with sharpened EBD tips in a plastic flat container with a Gel-Film onto which the cantilevers can be immobilized based on surface tension (plastic containers supplied from cantilever manufacturers can also be used). Then, store the container in the auto-dry cabinet. The shelf life is practically not limited (1–2 years).

**Preparation of mica and HOPG disks (modify)** ● **TIMING ~30 min**

▲ **CRITICAL** If you wish to use mica disks, go to Step 6. If you wish to use HOPG disks, go directly to Step 7. In general, mica substrate is used for depositing hydrophilic molecules, whereas HOPG substrate is used for hydrophobic samples such as crystalline cellulose.

**6|** Prepare a mica sheet (~10 × 100 $mm^2$) and cleave it to a thickness of less than 0.05 mm. Next, punch the thinly cleaved sheet using the puncher set to produce mica disks with a diameter of 1.5 mm. Go to Step 8.

▲ **CRITICAL STEP** The use of a thin mica sheet to produce disks is very important for achieving successful imaging, because disks punched out from a thicker mica sheet often have burrs at the edges and loosely packed layers. Such mica disks hamper imaging because of both low mechanical stability and contaminations.

**7|** Prepare HOPG sheets (~5 × 5 $mm^2$, <0.1 mm thick) by using a sharp knife. Punch them using the puncher to produce disks with a diameter of 2.0 mm. Much thinner HOPG disks are spontaneously produced from the punched HOPG disks and can be easily separated with a sewing needle.

▲ **CRITICAL STEP** Because HOPG is softer than mica, it is hard to make regularly shaped disks of diameters smaller than 2.0 mm. Again, the use of thin HOPG sheets for fabricating disks is very important in order to avoid low mechanical stability and contaminations.

**Preparation of sample stages** ● **TIMING more than 3 h (working time ~1 h)**

**8|** We use a glass rod (1.5 or 2.0 mm in diameter and 2 mm in height) as a sample stage[4,45]. Note that a larger diameter sample stage will produce a higher hydrodynamic pressure when it is moved fast, which perturbs the response of cantilever oscillation amplitude to tip-sample interaction[45,46]. Before use, clean glass rods with Kimwipes wetted with acetone, rinse them with Milli-Q water, place them on Kimwipes for drying, and then store them in a clean plastic box.

**9|** Under a stereoscopic microscope, glue either a mica disk or an HOPG disk onto the top of a sample stage using an epoxy adhesive. Then, wait for more than 3 h for drying.

▲ **CRITICAL STEP** The reverse side of a disk should be fully glued to the top surface of a sample stage to accomplish firm attachment.

■ **PAUSE POINT** After preparation, the sample stages with mica or HOPG disks can be stored in a clean plastic case. For convenience and time saving, prepare many sample stages with the disks at once.

**Preparation of lipid vesicles and mica-SLB (modify)** ● **TIMING ~3 h for vesicle preparation; variable for mica-SLB preparation**

▲ **CRITICAL** If you do not wish to use mica-supported planar lipid bilayers (mica-SLBs), directly go to Step 19. If you do wish to use mica-SLBs for specific or electrostatic immobilization of proteins, follow or adapt the following procedures (Steps 10–18). See reference 47.

**10|** *Preparation of lipid vesicles*. Dissolve each lipid compound in chloroform or in a mixture of chloroform, methanol and water in a glass tube (follow the instructions provided by the manufacturer). We used chloroform (100%) for dissolving DPPC, DPTAP and biotin-cap-DPPE. Store the lipid solutions at −20 °C.

**11|** Mix lipid solutions at a desired ratio in a glass tube. In the case of observing myosin V walking on actin filaments, a typical lipid composition is DPPC, DPTAP and biotin-cap-DPPE in a weight ratio of 0.85:0.05:0.1 (lipid composition A)[19].

**12|** Dry the organic solvent under a stream of $N_2$ gas, while warming up the glass tube by gripping it with your hand to facilitate solvent evaporation. To ensure full evaporation, leave the glass tube in a vacuum desiccator for at least 30 min.

**13|** Add a buffer solution to the glass tube (typical final concentration of lipids, 1 mg $ml^{-1}$), vortex it for ~30 s and sonicate it for ~3 min using the bath sonicator to disperse the lipids in the medium. At this stage, multilamellar lipid vesicles are formed. In the case of lipid composition A, we use Milli-Q water instead of a buffer solution.

**14|** Divide the lipid suspension into small aliquots (10 µl each in a 0.5-ml sample tube).
■ **PAUSE POINT** After preparation, the aliquots containing lipid vesicles can be stored at −80 °C before use.

**15|** *Preparation of mica-SLBs.* Thaw the multilamellar lipid vesicles stored at −80 °C by gripping the tube with your hand. Dilute the solution to 0.05–0.1 mg $ml^{-1}$ by adding a buffer solution. In the case of lipid composition A, we add a 10 mM $MgCl_2$ solution for the dilution.

**16|** To obtain small unilamellar vesicles, sonicate the multilamellar vesicle suspension (typically 100–150 µl) with the probe sonicator at intervals of 1 s with a duty ratio of ~0.5 until the suspension becomes transparent (typically no more than 30 cycles).

**17|** Deposit a drop (~2 µl) of the small unilamellar vesicle solution on freshly cleaved mica glued on a sample stage (prepared in Steps 8 and 9). Usually, we prepare 3–5 vesicle-deposited sample stages at once.

**18|** Put the vesicle-deposited sample stages in the sealed container, in the inside of which a Kimwipe wetted with Milli-Q water is stuffed. Incubate the vesicle-deposited sample stages until the mica surfaces are fully coated by lipid bilayers (**Fig. 6**). In the case of lipid composition A, the incubation time is more than 3 h (typically overnight) after the deposition. The container can maintain high humidity to avoid sample drying. To keep the sample stages from falling, place them on the Gel-Film glued on a glass slide (**Fig. 6c**). The sealed container should be used upside down so that the sample stages are easily handled with tweezers. The details of other useful lipid compositions, practical methods to prepare mica-SLBs and their application to several samples are well described elsewhere[35].
■ **PAUSE POINT** After preparation, mica-SLBs on the sample stages can be stored in the sealed container for up to 3 d at room temperature (25 °C).

**Preparation and mounting of the AFM liquid cell ● TIMING ~10 min**

**19|** Clean the AFM liquid cell equipped with the cantilever holder by using a piece of Super cloth containing mild detergent, and then rinse it abundantly with tap water. Sonicate it for 3 min in a beaker filled with tap water and further rinse it repeatedly with Milli-Q water. Then, place it on a Kimwipe and dry it using a rubber hand blower.

**20|** Clamp a small cantilever to the cantilever holder as shown in **Figure 7a**.
▲ **CRITICAL STEP** The cantilever should be tightly clamped into the holder, otherwise unwanted vibrations and insufficient feedback control will result (**Fig. 7**)[46].

**21|** Mount the AFM liquid cell on the high-speed AFM apparatus. Gently wash the liquid cell 2–3 times using an imaging buffer (~60 µl) to remove dirt, while sucking the buffer using a peristaltic pump. Next, fill the liquid cell with the imaging buffer (~60 µl).
**!** **CAUTION** Do not fill the liquid cell with more than 60 µl of imaging buffer. Otherwise, the *z*-piezo to be mounted later will get wet and result in a short circuit and thus in fatal damage when high voltage is applied.
▲ **CRITICAL STEP** After this step and until the end of AFM measurement, keep the cantilever from drying. Dirt contaminants tend to be accumulated on the cantilever during drying by water evaporation.

**Laser alignment ● TIMING ~3 min**

**22|** Align the laser focusing position relative to the cantilever by moving both lateral and vertical positions of the cantilever holder so that the intensity of light reflected back from the cantilever is maximized (**Fig. 8** and **Supplementary Video 1**).

**23|** Adjust the photodetector position so that the reflected laser guided to the photodetector makes a spot at its center (**Supplementary Video 1**).

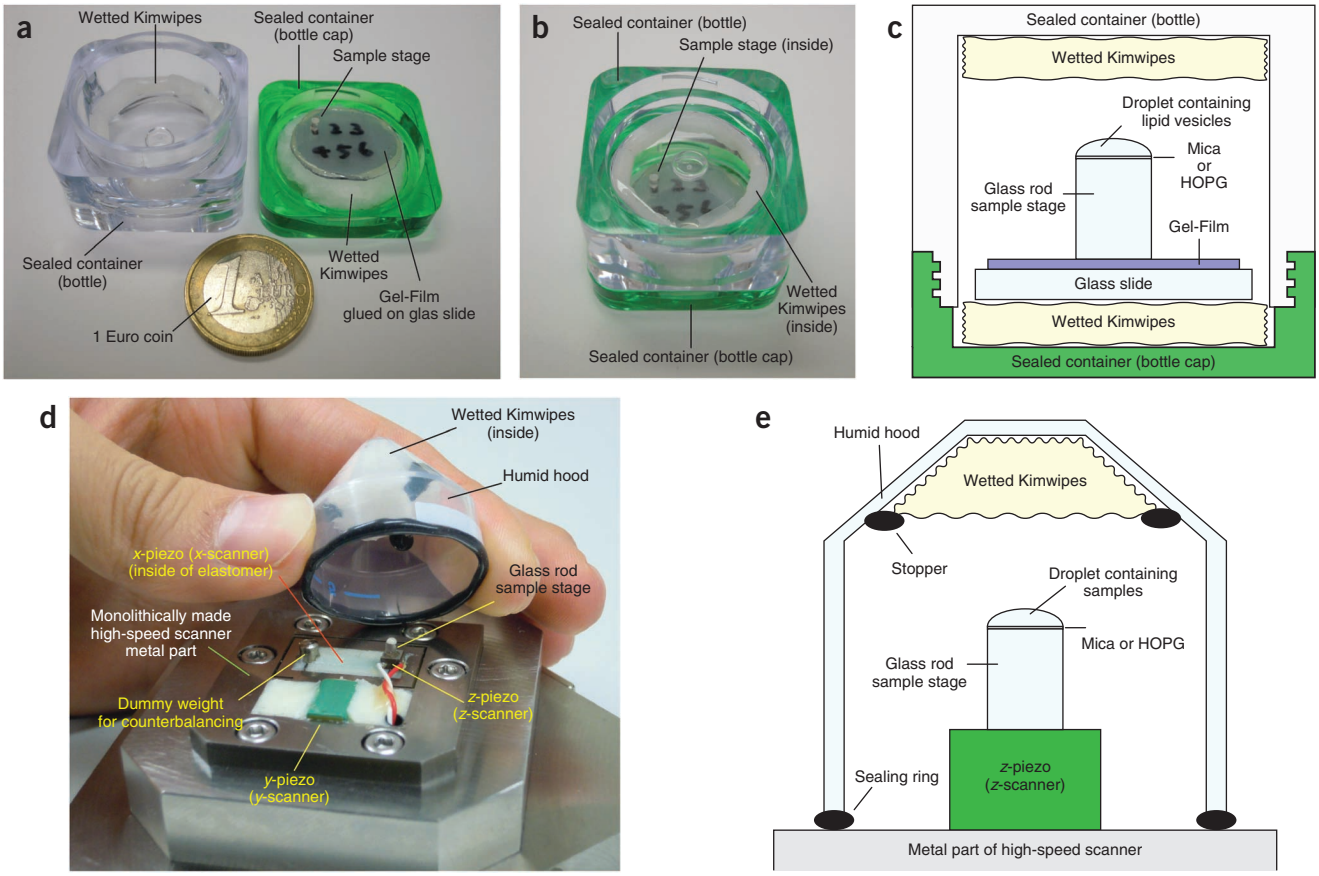


**Figure 6** | Storage tools used to preserve a solution droplet on the sample stage without drying it. (**a**) Photograph showing an opened container containing sample stages (note that the sample stages are placed in the bottle cap). (**b**) Photograph showing the sealed container. (**c**) Schematic showing the sealed container. (**d**) Photograph showing a humid hood used during incubation of solution on a sample stage glued onto the *z*-piezo. (**e**) Schematic showing the humid hood covered over the sample stage glued onto the *z*-piezo.



### Cleaning of the *z*-piezo surface ● TIMING ~1 min

**24|** Clean the surface of the *z*-piezo (z-scanner) with a piece of Super cloth wetted with acetone to remove any dust and to confirm the flatness of the *z*-piezo surface.

### Sample deposition on the substrate (modify) ● TIMING ~15–30 min

**25|** Procedures for sample deposition onto a substrate surface depend on the surface to be used. For sample deposition onto mica-SLBs with biotin (for example, acto-myosin V) go directly to Step 28C. For other types of sample deposition (for example, rotorless $F_1$-ATPase and cellulose + cellulase), perform Steps 26 and 27 first, and then choose the appropriate option in Step 28.

**26|** Place a drop of nail polish on the top of *z*-piezo. Immediately after that, place a sample stage with a glued mica or HOPG disk on the top of the *z*-piezo using tweezers and wait for 10 min until the sample stage is firmly fixed on the *z*-piezo.
▲ CRITICAL STEP To avoid contamination, do not touch the sample stage except when placing the *z*-piezo.

**27|** Cleave a few top layers of the mica or HOPG using adhesive tape (e.g., Scotch tape) to have a clean surface. If you cannot cleave the surface anymore, remove the glass stage from the *z*-piezo and go to the recycling process (Step 45), and then repeat Steps 24–27.

**28|** For direct sample deposition onto a bare surface of mica or HOPG, go to option A. For covalent immobilization of proteins onto a mica surface with glutaraldehyde, go to option B. To observe walking myosin V, go to option C (proceed directly from Step 25).
▲ CRITICAL STEP Carefully inspect that the mica or HOPG surface shows a clean surface without burrs after the cleavage.

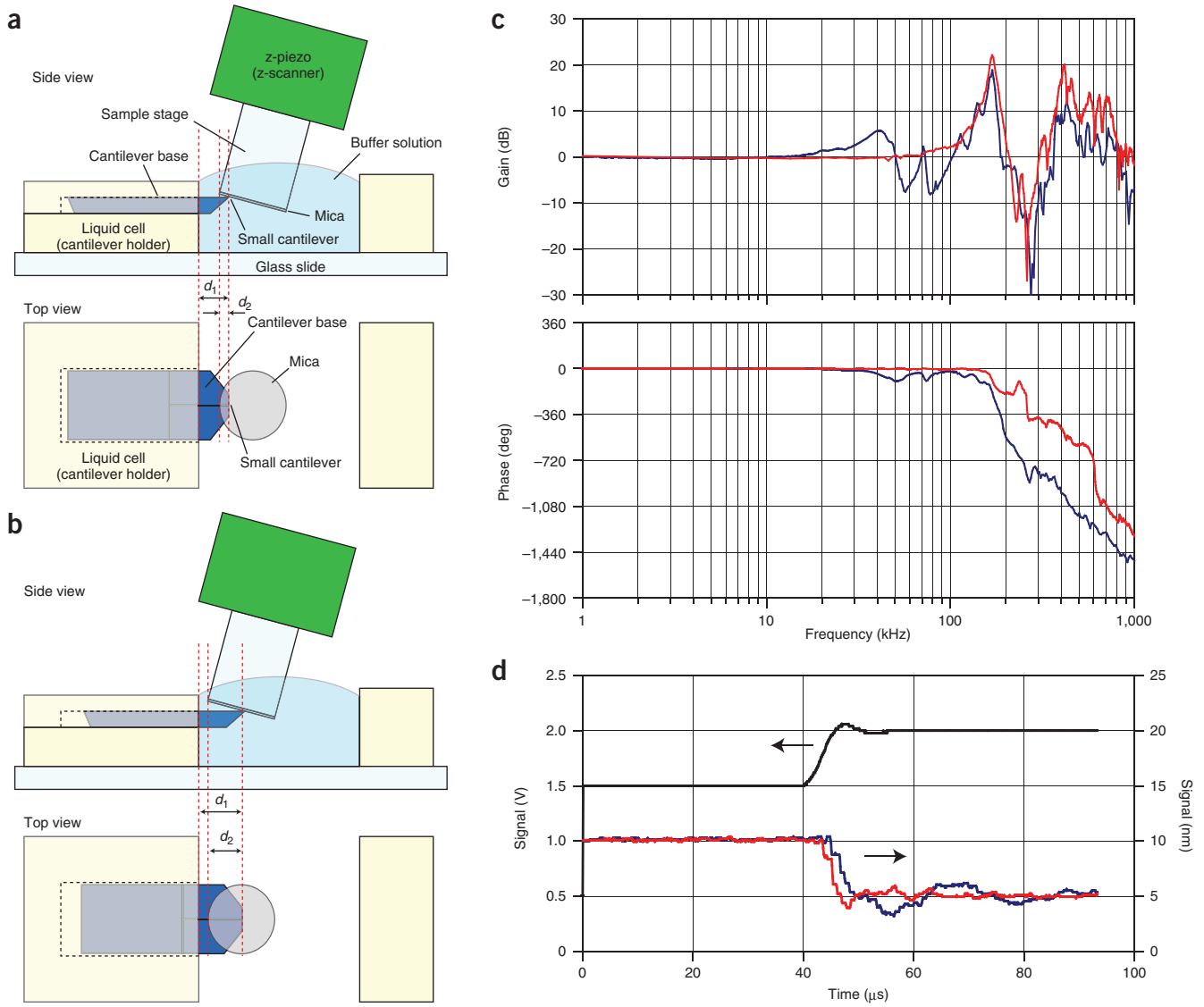




**Figure 7** | Importance of firmly mounting the cantilever base and selecting the imaging region for successful imaging. (**a**) Schematic showing appropriate imaging region selection and holding of the cantilever base. The cantilever base is deeply inserted into the cantilever holder. The imaging region locates at an outer area of the mica disk. The distances of $d_1$ and $d_2$ shown should be less than 1 mm and 0.2–0.3 mm, respectively. (**b**) Schematic showing inappropriate imaging region selection and holding of the cantilever base. (**c**) Frequency responses of the sinusoidally driven *z*-scanner displacement detected by deflection of a small cantilever whose tip is in contact with the sample stage. The red and navy blue curves show the responses detected in the appropriate setting shown in **a** and in the inappropriate setting shown in **b**, respectively. The peaks at 171 kHz indicate the first resonant frequency of the *z*-scanner. Note that the *z*-scanner is actually moving in the same way for both **a** and **b**, but in the setting shown in **b** the cantilever as a sensor cannot precisely detect the *z*-scanner movement, because the cantilever chip itself is moved by a hydrodynamic pressure produced by *z*-scanner movement. (**d**) Amplitude responses of an oscillating cantilever to *z*-piezo movement. The cantilever tip is in contact with the sample stage. Black curve shows a signal input to the *z*-piezo; the red curve shows the response in setting **a**; the navy-blue curve shows the response in the setting **b** (considerable delay occurs in the response).

### (A) Deposition directly onto bare mica or HOPG surface ● TIMING ~5 min

(i) Deposit a drop of sample solution onto the freshly cleaved surface, cover the sample stage with a humid hood (**Fig. 6d,e**), and wait for a while (typically 3 min). After that, rinse the deposited sample with an appropriate buffer solution to remove any excess of molecules (**Supplementary Video 2**). Go to HS-AFM imaging (Step 29). In the case of observations of cellulase on cellulose on an HOPG substrate[23], 2 μl of cellulose suspension in water (0.1–0.5% (vol/vol)) was dropped on the freshly cleaved HOPG surface and incubated for 5–10 min. Then the solution was rinsed with 18 μl of buffer A before AFM imaging (cellulase was added while imaging was going on).

▲ CRITICAL STEP Avoid drying of the sample solution on the substrate disk in order to prevent degeneration of the biomolecules attached to the substrate surface.

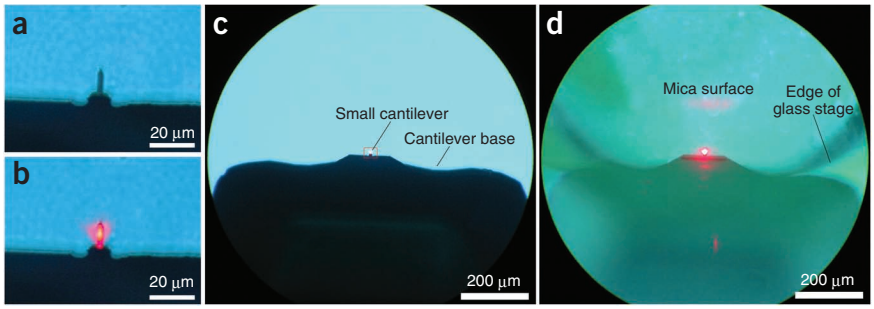


**Figure 8** | Optical microscopic views of a small cantilever. (**a**,**b**) Magnified views of a small cantilever without incident laser (**a**) and with incident laser (**b**). (**c**,**d**) Low-magnified views of the cantilever when the mica surface is far from the cantilever (**c**) and when the surface is close to the cantilever (**d**).

**(B) Covalent immobilization of proteins onto a mica surface with glutaraldehyde ● TIMING ~12 min**

▲ **CRITICAL STEP** This immobilization method has been applied to observe rotary catalysis of the $\alpha_3\beta_3$ subcomplex of $F_1$-ATPase with Lys-tag at the N terminus[22]. Therefore, we here describe the procedure to immobilize this protein. However, the procedure should be adaptable for many other proteins with amino groups on their outer surfaces, although the orientation of the immobilized molecules is mainly determined by the position of the most reactive amino group.

(i) Deposit a drop (~2 μl) of 3-aminopropyl-triethoxysilane (0.05–0.1% (vol/vol) in Milli-Q water) on a freshly cleaved mica surface, cover the sample stage with a humid hood (**Fig. 6d**,**e**), wait for 3 min, and rinse the surface (**Supplementary Video 2**) with Milli-Q water.
▲ **CRITICAL STEP** The preparation of a diluted 3-aminopropyl-triethoxysilane solution should be done just before deposition because the aminosilane quickly reacts with water.

(ii) Deposit a drop (~2 μl) of glutaraldehyde (diluted to 0.1–0.25% (wt/vol) with Milli-Q water), cover the sample stage with a humid hood (**Fig. 6d**,**e**), wait for 3 min, and rinse the surface (**Supplementary Video 2**) with a buffer solution containing no primary amine (we used 10 mM HEPES/NaOH (pH 7.4), 10 mM KCl, 5 mM $MgSO_4$).

(iii) Deposit a drop (~2 μl) of protein solution (1–10 nM, in a buffer containing no primary amine), cover the sample stage with a humid hood (**Fig. 6d**,**e**), wait for 5 min, and then rinse the surface (**Supplementary Video 2**) with a buffer solution containing a reagent with primary amine (we used 10 mM Tris-HCl (pH 8.0)) to terminate residual active glutaraldehyde on the surface.

(iv) After that, we can use any buffer solutions to observe the protein molecules immobilized on the surface (we used buffer B for observing the $\alpha_3\beta_3$ subcomplex of $F_1$-ATPase). Proceed to HS-AFM imaging (Step 29).
▲ **CRITICAL STEP** Avoid drying of the sample solution on the substrate disk in order to prevent degeneration of the biomolecules attached to the substrate surface.

**(C) Deposition for observing walking myosin V ● TIMING ~20 min**

(i) From the sealed container, take a sample stage with mica on the top of which SLBs are formed (**Fig. 6a–c**).

(ii) Place a drop of nail polish on the top of the *z*-piezo. Immediately after that, place the sample stage on the top of the *z*-piezo by using tweezers. After that, immediately cover the humid hood over the sample stage as shown in **Figure 6d**,**e**.
▲ **CRITICAL STEP** Do not dry the planar lipid bilayers on mica, or most of the bilayers will certainly be damaged. These procedures should therefore be performed quickly (ideally, within 1 min).

(iii) Rinse the sample surface (**Supplementary Video 2**) with Milli-Q water dropwise (20 μl × 5) and replace the solution with buffer C. Then, deposit a drop (2 μl) of streptavidin (1 μg $ml^{-1}$) in buffer C on the bilayer surface, cover the sample stage with a humid hood (**Fig. 6d**,**e**), and then wait for 3 min.
▲ **CRITICAL STEP** Rinse the sample thoroughly for removing the residual vesicles.

(iv) After rinsing with buffer C (20 μl × 3), deposit a drop (2 μl) of partially biotinylated actin filaments that are stabilized with phalloidin (~1 μM in buffer C) on the bilayer surface, cover the sample stage with a humid hood (**Fig. 6d**,**e**), and then wait for 10 min.
▲ **CRITICAL STEP** Rinse the sample thoroughly to remove the residual streptavidin.

(v) After rinsing with buffer C (20 μl), deposit a drop (2 μl) of myosin V-HMM solution (0.1–1 nM) on the bilayer surface, cover the sample stage with a humid hood (**Fig. 6d**,**e**), and wait for 3 min. At this point, the sample stage becomes firmly fixed on the *z*-piezo. Go to HS-AFM imaging (Step 29).
▲ **CRITICAL STEP** In order to avoid contamination, do not touch the sample surface. By using the humid hood (**Fig. 6d**,**e**), maintain the sample surface covered with a buffer solution so as not to degenerate the molecules on the surface.
**? TROUBLESHOOTING**

**High-speed AFM imaging (approach) ● TIMING ~5 min**

**29|** Mount the scanner, with the z-scanner attached to the sample stage with a sample to observe, over the liquid cell containing a buffer solution (**Supplementary Video 3**).

**! CAUTION** Make sure that the top of the sample stage is sufficiently far away from the cantilever to avoid crashing. If it crashes, the cantilever is often damaged and all previous procedures have to be repeated.

**30|** Adjust the scanner position so that the cantilever tip is positioned near the substrate disk (**Fig. 8** and **Supplementary Video 3**).
▲ **CRITICAL STEP** Positioning of the lever portion of the cantilever to a region near the substrate disk edge is crucial to avoid disturbance of the amplitude measurement by low frequency vibrations of the lever and cantilever chip itself, which are produced by a hydrodynamic pressure[45,46].

**31|** Execute a coarse approach while carefully watching the cantilever and the substrate disk surface on the digital camera (or CCD camera) display. Once the substrate disk surface is seen on the monitor, stop the approach.
▲ **CRITICAL STEP** To avert a crash, this careful watching and quick halting of the coarse approach is very important. It is always better to halt the coarse approach before a clear view of the substrate disk surface appears.

**32|** Measure a thermal fluctuation spectrum of the cantilever using the fast Fourier transform (FFT) analyzer (in the HS-AFM software) to find the first resonant frequency of the cantilever.

**33|** Apply sinusoidal AC voltage to a piezo actuator fixed in the cantilever holder to excite the cantilever at the measured resonant frequency.

**34|** Adjust the cantilever oscillation amplitude to 0.1–0.5 V while looking at the oscillation signal on an oscilloscope screen (typical amplitude: 1–5 nm; the amplitude in nm cannot be exactly known before calibrating the optical lever sensitivity. See Step 43).

**35|** Adjust the amplitude detector gain to have its output of 0.1–0.5 V.

**36|** Adjust the set point voltage of the PID controller to ~60–70% of the amplitude detector output voltage, and then switch on the PID controller. Upon switching on, the *z*-piezo becomes fully extended because the cantilever tip is not yet in contact with the sample surface.

**37|** While carefully checking both PID output and cantilever amplitude signal, execute slow approach until the computer automatically stops the approach upon detecting tip-sample contact (a software program is always monitoring both the amplitude and PID output).
▲ **CRITICAL STEP** When the cantilever is approaching the sample surface, the oscillation amplitude usually increases first (due to an unspecified effect). Readjust the set point voltage of the PID controller to ~60–70% of the amplitude detector output voltage.
**? TROUBLESHOOTING**

**38|** After the approach is automatically halted, adjust the *z*-piezo position by changing the bias DC voltage of the *z*-piezo driver so that the PID output voltage becomes around 0 V. Slowly increase the integral gain of the PID controller until the feedback signal starts to oscillate. Then slightly decrease the gain so that the oscillation ceases. Do likewise for the proportional gain and the derivative gain.

**High-speed AFM imaging (imaging) ● TIMING usually 2–5 h**
**39|** Before starting imaging, increase the set point voltage of the PID controller to ~95% of the free oscillation amplitude.

**40|** Start imaging. At first you will obtain noisy images like the one shown in **Figure 9** (0.15 s) and **Supplementary Video 4**. Slowly decrease the set point voltage of the PID controller until clearer images appear (**Fig. 9**, 2.94–3.24 s). Owing to 'tip parachuting' (i.e., complete detachment of the cantilever tip from the sample surface at the downhill regions of the sample), noisy lines extending to the plus *x*-direction (imaging direction) appear in the images. In this stage, you can choose one of the following two operations to obtain clear images like those shown in **Figure 9** (6.33–11.92 s) and **Supplementary Video 4**. Further decrease the set point voltage or switch the PID controller from the conventional mode to the dynamic PID control mode[8] and then adjust the gain that is especially equipped for this mode in addition to the PID gains. In this mode, the PID gain is unchanged for the uphill regions of the sample but is increased for the downhill regions[8]. The effect of the dynamic PID control mode is shown in **Supplementary Video 5**. The choice depends on the fragility of your sample. For samples with higher fragility, the latter operation should be chosen.

**41|** When no improvement is attained in the image quality, change the cantilever chip to a new one, because noisy images are usually due to tip smear. When the image quality is good enough, move to the next steps.
**? TROUBLESHOOTING**

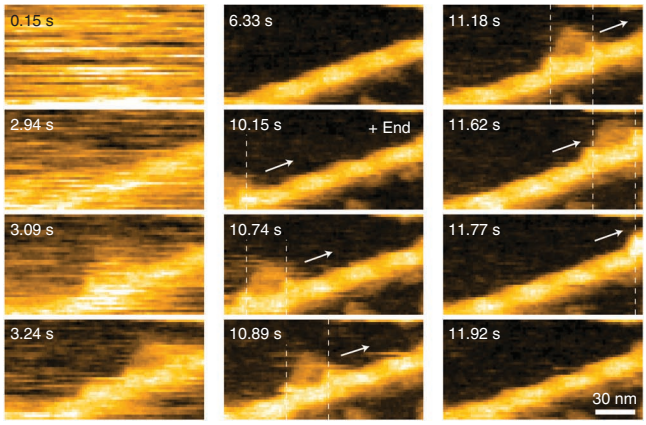


**Figure 9** | Clipped high-speed AFM images showing relationship between applying tapping force and image quality. From 0.15 s to 3.24 s, tapping force was gradually increased. In other words, the set point voltage of the PID controller was gradually decreased to increase the tapping force. Next, appropriate objects, depending on the particular experiment (in this case, actin filaments), are searched by laterally moving the sample stage by changing the offset DC voltages of the piezo-driver for the *x*- and *y*-scanners. In this model experiment, myosin V–HMM movement (from bottom left to top right) along an actin filament was observed (see the arrows). Imaging rate, 6.8 fps; scan size, 150 × 75 nm$^2$; number of pixels, 80 × 40; *z*-scale, 10 nm.

**42|** Find target molecules by scanning different areas (change the offset DC voltages of the *x*- and *y*-piezo drivers) and readjust imaging parameters (cantilever oscillation amplitude, excitation frequency and set point voltage) until high-resolution images appear (**Figs. 10** and **11**; **Supplementary Video 4**).
▲ **CRITICAL STEP** The AFM tip often picks up contaminants, which considerably deteriorates the image quality. When this occurs, repeatedly vary the set-point voltage within a certain range while imaging. By this operation, the cantilever tip interacts with the sample strongly and weakly. This procedure can sometimes remove attached contaminants and improves the image quality (**Fig. 11**). It is advisable to scan over a wider area and to use a faster frame rate to increase the tip-sample interaction, which might be effective for removing attached contaminations from the AFM tip. After capturing enough images, switch off both the PID controller and the wave generator used for exciting the cantilever.

**43|** Measure force curves to calibrate the OBD detection sensitivity[48].
▲ **CRITICAL STEP** To know the cantilever oscillation amplitude not in voltage but in nm, calibration should have been done before starting imaging experiments. However, because force curve measurements are apt to damage the cantilever tip, we often make this calibration after completing imaging. The OBD detection sensitivity does not change much as long as the same type of cantilever is used.

**44|** Release the sample surface from the cantilever tip using the stepper motor used for the tip approach.

**Recycling of glass stages ● TIMING ~1 d**
**45|** After finishing the imaging experiments, remove the sample stage from the *z*-piezo using acetone. Then immerse the used sample stages in nondiluted sulfuric acid to remove adhesives and clean the glass rods.
**! CAUTION** Never detach the glass rod by applying force, or the *z*-piezo will be damaged.
▲ **CRITICAL STEP** Put drops of acetone around the interface between the *z*-piezo and the glass rod and wait until the glass rod naturally detaches from the *z*-piezo.

**Recycling of cantilevers ● TIMING ~1 d**
**46|** After use, rinse the cantilevers with Milli-Q water. To remove the EBD tip and contaminants from the cantilevers, apply RF argon/oxygen plasma etching to the cantilever over 1 d. Typical power of the RF plasma is about 20 W and the gas pressure is ~180 mTorr.

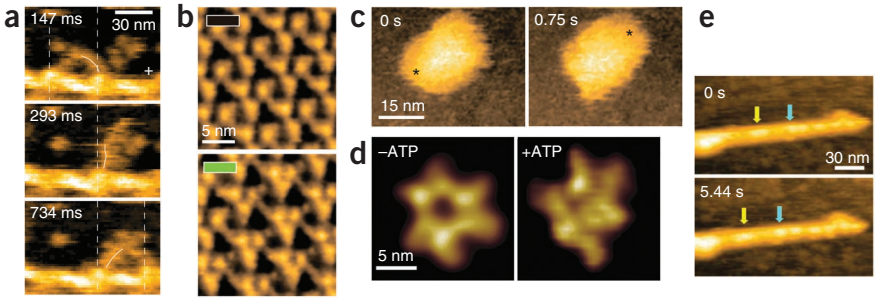


**Figure 10** | High-speed AFM images of proteins in action. (**a**) Swinging lever arm motion at the leading head of myosin V–HMM on an actin filament[19]. The '+' symbol indicates the plus end of the actin filament. (**b**) bR in response to light (black and green bars indicate dark and light illumination conditions, respectively)[20]. (**c**) Alternate binding of GroES (marked with the asterisks) to two rings of GroEL[34]. (**d**) ATP-induced conformational change of β-subunits in rotorless $F_1$-ATPase ($\alpha_3\beta_3$ subcomplex)[22]. (**e**) Cellulase moving left while hydrolyzing cellulose fibers[23]. Each arrow (yellow or blue) indicates the position of a cellulose molecule.

**? TROUBLESHOOTING**
**Sample preparation (Step 28C)**
When you are not yet used to the sample deposition, you should confirm whether or not each step for sample preparation (e.g., lipid-bilayer preparation, streptavidin deposition, actin deposition) is successful by imaging the sample surface with HS-AFM after each step is done.

**Tip approach (Step 37)**
You may have a difficulty in executing the slow approach because of oscillation of the PID controller or reduction

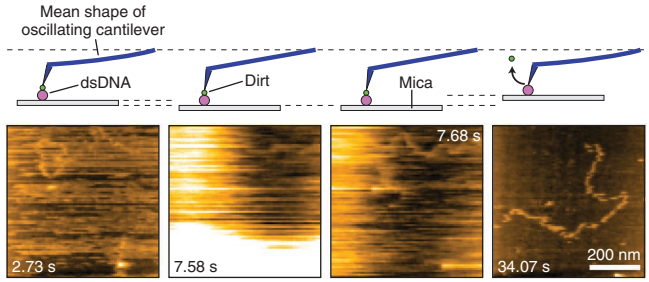


**Figure 11** | Effect of AFM tip smear and its removal on image quality. Top, schematics illustrate the speculated respective situations from the respective AFM images. Improvement of the image quality of double-stranded DNA (dsDNA) is demonstrated. The *z*-positions of a substrate disk are indicated with broken lines drawn nearby. At 2.73 s, the AFM tip picked up contaminants, resulting in a blurred image. By varying the set point voltage of the PID controller, the image quality drastically improved (rightmost image). Imaging rate, 9.9 fps; scan size, 600 × 600 nm$^2$; *z*-scale, 3.5 nm.

of the reflected laser power. When this problem is encountered, you should check the fixing of the glass stage on the *z*-piezo, inspect the mica disk or readjust the sample position relative to the cantilever tip (**Fig. 7**).

### Imaging (Step 41)

When no improvement is attained in the image quality even after changing the cantilever once or twice, at least one step in previous procedures has not been done appropriately. It is difficult to find a cause for noisy images. The best troubleshooting is to conduct each step as described in this protocol, particularly with respect to the indicated critical steps. For samples that we have imaged many times (such as myosin V and rotorless $F_1$-ATPase), we can obtain fairly good images with a success rate of over 80%. However, whether or not we can capture high-quality images largely depends on the tip condition. Accordingly, we often change the cantilever chips one after another until we can acquire high-quality images.

## ● TIMING

Steps 1–5, fabrication of cantilever tips: 3–5 h (depending on the number of cantilevers)
Steps 6 and 7, preparation of mica and HOPG disks: ~30 min
Steps 8 and 9, preparation of sample stages: more than 3 h (working time ~1 h)
Steps 10–14, preparation of lipid vesicles: ~3 h
Steps 15–18, preparation of mica-SLBs: variable, depending on lipid compositions (typical working time, ~15 min)
Steps 19–21, preparation and mounting of the AFM liquid cell: ~10 min
Steps 22 and 23, laser alignment: ~3 min
Step 24, cleaning of the *z*-piezo surface: ~1 min
Steps 25–28, sample deposition on the substrate: ~15–30 min
Steps 29–38, high-speed AFM imaging (approach): ~5 min
Steps 39–44, high-speed AFM imaging (imaging): usually 2–5 h
Step 45, recycling of glass stages: ~1 d
Step 46, recycling of cantilevers: ~1 d

## ANTICIPATED RESULTS

HS-AFM is a new method for directly obtaining visual information on dynamics of functioning proteins. For instance, the following dynamics have thus far been successfully captured on video: the myosin V lever arm swing at the leading head after trailing head detachment from actin (**Fig. 10a**)[19], the structural change of bR upon green light illumination (**Fig. 10b**)[20,21], alternate binding of GroES to the two rings of GroEL (**Fig. 10c**)[34], the structural change of rotorless $F_1$-ATPase during ATP hydrolysis (**Fig. 10d**)[22], the processive run of cellulase on crystalline cellulose fibers (**Fig. 10e**)[23], the dynamics of bR 2D crystals[24], amyloid-like fibril formation from lithostathine[25], the wiggling motion of intrinsically disordered regions of FACT protein[26], the membrane-mediated interaction between c-rings of ATP synthase[27], and the dynamics of nucleosomes[28]. Although it is only imaged from the top direction, the whole topography of a protein molecule and its minute temporal changes can be visualized with HS-AFM. Unlike fluorescence microscopy, various dynamic events of molecules appear in an AFM video without planned selection, meaning that both expected and unexpected dynamic molecular behaviors can appear simultaneously. Therefore, we have a great chance of learning the details of several facts of molecular action in one imaging experiment. Moreover, the molecular action that appears on video can often be interpreted in a straightforward manner without sophisticated analysis, thereby helping to obtain convincing conclusions. These excellent general features of HS-AFM imaging markedly facilitate and accelerate our understanding of the functional mechanisms of proteins.

*Note: Supplementary information is available in the online version of the paper.*

**ACKNOWLEDGMENTS** We thank D. Yamamoto for technical assistance. This work was supported by the Core Research for Evolutionary Science and Technology (CREST) program of the Japan Science and Technology Agency (JST); a Grant-in-Aid for Basic Research (S) from the Japan Society for the Promotion of Science (JSPS) (no. 20221006); a Grant-in-Aid for Scientific Research on Innovative Areas (Research in a proposed Research Area) from the Ministry of Education, Culture, Science, Sports and Technology (MEXT)-Japan; and the Knowledge Cluster Initiative/MEXT-Japan.

**AUTHOR CONTRIBUTIONS** All the authors designed and discussed the experiments. T.U. and N.K. equally contributed to this work, conducted the experiments, prepared all figures and movies, and drafted the MATERIALS and PROCEDURE sections. T.A. wrote the introductory part of manuscript and edited the whole manuscript.

**COMPETING FINANCIAL INTERESTS** The authors declare no competing financial interests.

Published online at http://www.nature.com/doifinder/10.1038/nprot.2012.047. Reprints and permissions information is available online at http://www.nature.com/reprints/index.html.



1. Müller, D.J. & Engel, A. Atomic force microscopy and spectroscopy of native membrane proteins. *Nat. Protoc.* **2**, 2191–2197 (2007).
2. Viani, M.B. *et al.* Fast imaging and fast force spectroscopy of single biopolymers with a new atomic force microscope designed for small cantilevers. *Rev. Sci. Instrum.* **70**, 4300–4303 (1999).
3. Viani, M.B. Probing protein-protein interactions in real time. *Nat. Struct. Biol.* **7**, 644–647 (2000).
4. Ando, T. *et al.* A high-speed atomic force microscope for studying biological macromolecules. *Proc. Natl. Acad. Sci. USA* **98**, 12468–12472 (2001).
5. Kitazawa, M., Shiotani, K. & Toda, A. Batch fabrication of sharpened silicon nitride tips. *Jpn. J. Appl. Phys.* **42**, 4844–4847 (2003).
6. Kodera, N., Yamashita, H. & Ando, T. Active damping of the scanner for high-speed atomic force microscopy. *Rev. Sci. Instrum.* **76**, 053708 (2005).
7. Ando, T. *et al.* High-speed atomic force microscopy for studying the dynamic behavior of protein molecules at work. *e-J. Surf. Sci. Nanotechnol.* **3**, 384–392 (2005).
8. Kodera, N., Sakashita, M. & Ando, T. Dynamic proportional-integral-differential controller for high-speed atomic force microscopy. *Rev. Sci. Instrum.* **77**, 083704 (2006).
9. Uchihashi, T., Kodera, N., Itoh, H., Yamashita, H. & Ando, T. Feed-forward control for high-speed AFM imaging of biomolecules. *Jpn. J. Appl. Phys.* **45**, 1904–1908 (2006).
10. Ando, T. *et al.* High-speed atomic force microscopy for studying the dynamic behavior of protein molecules at work. *Jpn. J. Appl. Phys.* **45**, 1897–1903 (2006).
11. Uchihashi, T., Yamashita, H. & Ando, T. Fast phase imaging in liquids using a rapid scan atomic force microscope. *Appl. Phys. Lett.* **89**, 213112 (3 pp) (2006).
12. Yamashita, H. *et al.* Tip-sample distance control using photo-thermal actuation of a small cantilever for high-speed atomic force microscopy. *Rev. Sci. Instrum.* **78**, 083702 (2007).
13. Fukuma, T., Okazaki, Y., Kodera, N., Uchihashi, T. & Ando, T. High resonance frequency force microscopy scanner using inertia balance support. *Appl. Phys. Lett.* **92**, 243119 (2008).
14. Ando, T. *et al.* High-speed AFM and nano-visualization of biomolecular processes. *Pflügers Archiv.—Eur. J. Physiol.* **456**, 211–225 (2008).
15. Ando, T., Uchihashi, T. & Fukuma, T. High-speed atomic force microscopy for nano-visualization of dynamic biomolecular processes. *Prog. Surf. Sci.* **83**, 337–437 (2008).
16. Casuso, I., Rico, F. & Scheuring, S. High-speed atomic force microscopy: structure and dynamics of single proteins. *Curr. Opin. Chem. Biol.* **15**, 704–709 (2011).
17. Katan, A.J. & Dekker, C. High-speed AFM reveals the dynamics of single biomolecules at the nanometer scale. *Cell* **147**, 979–982 (2011).
18. Ando, T. High-speed atomic force microscopy coming of age. *Nanotechnology* **23**, 062001 (27 pp) (2012).
19. Kodera, N., Yamamoto, D., Ishikawa, R. & Ando, T. Video imaging of walking myosin V by high-speed atomic force microscopy. *Nature* **468**, 72–76 (2010).
20. Shibata, M. *et al.* High-speed atomic force microscopy shows dynamic molecular processes in photo-activated bacteriorhodopsin. *Nat. Nanotechnol.* **5**, 208–212 (2010).
21. Shibata, M., Yamashita, H., Uchihashi, T., Kandori, H. & Ando, T. Structural changes in bacteriorhodopsin in response to alternate illumination observed by high-speed atomic force microscopy. *Angew. Chem. Int. ed.* **50**, 4410–4413 (2011).
22. Uchihashi, T., Iino, R., Ando, T. & Noji, H. High-speed atomic force microscopy reveals rotary catalysis of rotorless $F_1$-ATPase. *Science* **333**, 755–758 (2011).
23. Igarashi, K. *et al.* Traffic jams reduce hydrolytic efficiency of cellulase on cellulose surface. *Science* **333**, 1279–1282 (2011).
24. Yamashita, H. *et al.* Dynamics of bacteriorhodopsin 2D crystal observed by high-speed atomic force microscopy. *J. Struct. Biol.* **167**, 153–158 (2009).
25. Milhiet, P.-E. *et al.* Deciphering the structure, growth and assembly of amyloid-like fibrils using high-speed atomic force microscopy. *PLoS ONE* **5**, e13240 (8 pp) (2010).
26. Miyagi, A. *et al.* Visualization of intrinsically disordered regions of proteins by high-speed atomic force microscopy. *Chem. Phys. Chem.* **9**, 1859–1866 (2008).
27. Casuso, I., Sens, P., Rico, F. & Scheuring, S. Experimental evidence for membrane-mediated protein-protein interaction. *Biophys. J.* **99**, L47–L49 (2010).
28. Miyagi, A., Ando, T. & Lyubchenko, Y.L. Dynamics of nucleosomes assessed with time-lapse high-speed atomic force microscopy. *Biochemistry* **59**, 7901–7908 (2011).
29. Sanchez, H., Suzuki, Y., Yokokawa, M., Takeyasu, K. & Wyman, C. Protein-DNA interactions in high speed AFM: single molecule diffusion analysis of human RAD54. *Integr. Biol.* **3**, 1127–1134 (2011).
30. Suzuki, Y. *et al.* Visual analysis of concerted cleavage by type IIF restriction enzyme SfiI in subsecond time region. *Biophys. J.* **101**, 2992–2998 (2011).
31. Wickham, S.F.J. *et al.* Direct observation of stepwise movement of a synthetic molecular transporter. *Nat. Nanotechnol.* **6**, 166–169 (2011).
32. Inoue, S., Uchihashi, T., Yamamoto, D. & Ando, T. Direct observation of surfactant aggregate behavior on a mica surface using high-speed atomic force microscopy. *Chem. Commun.* **47**, 4974–4976 (2011).
33. Giocondi, M.-C. *et al.* Surface topography of membrane domains. *Biochim. Biophys. Acta.-Biomembranes* **1798**, 703–718 (2010).
34. Yamamoto, D., Nagura, N., Omote, S., Taniguchi, M. & Ando, T. Streptavidin 2D crystal substrates for visualizing biomolecular processes by atomic force microscopy. *Biophys. J.* **97**, 2358–2367 (2009).
35. Yamamoto, D. *et al.* High-speed atomic force microscopy techniques for observing dynamic biomolecular processes. *Methods Enzymol.* **475** (Part B): 541–564 (2010).
36. Lyubchenko, Y.L., Shlyakhtenko, L.S. & Ando, T. Imaging of nucleic acids with atomic force microscopy. *Methods* **54**, 274–283 (2011).
37. Yamamoto, D., Uchihashi, T., Kodera, N. & Ando, T. Anisotropic diffusion of point defects in two-dimensional crystal of streptavidin observed by high-speed atomic force microscopy. *Nanotechnol.* **19**, 384009 (9 pp) (2008).
38. Yokokawa, M *et al.* Fast-scanning atomic force microscopy reveals the ATP/ADP-dependent conformational changes of GroEL. *EMBO J.* **25**, 4567–4576 (2006).
39. Fantner, G.E., Barbero, R.J., Gray, D.S. & Belcher, A.M. Kinetics of antimicrobial peptide activity measured on individual bacterial cells using high-speed atomic force microscopy. *Nat. Nanotechnol.* **5**, 280–285 (2010).
40. Sakamoto, T. *et al.* Direct observation of processive movement by individual myosin V molecules. *Biochem. Biol. Res. Commun.* **272**, 586–590 (2001).
41. Koide, H. *et al.* Identification of the specific IQ motif of myosin V from which calmodulin dissociates in the presence of $Ca^{2+}$. *Biochemistry* **45**, 11598–11604 (2006).
42. Spudich, J.A. & Watt, S. The regulation of rabbit skeletal muscle contraction. *J. Biol. Chem.* **246**, 4866–4871 (1971).
43. Araki, J. *et al.* Flow properties of microcrystalline cellulose suspension prepared by acid treatment of native cellulose. *Colloid Surface A* **142**, 75–82 (1998).
44. Igarashi, K. *et al.* Surface density of cellobiohydrolase on crystalline celluloses. A critical parameter to evaluate enzymatic kinetics at a solid-liquid interface. *FEBS J.* **273**, 2869–2878 (2006).
45. Ando, T. *et al.* A High-speed atomic force microscope for studying biological macromolecules in action. *Jpn. J. Appl. Phys.* **41**, 4851–4856 (2002).
46. Ando, T. & Uchihashi, T. High-speed AFM and imaging of biomolecular processes In *Nanoscale Liquid Interfaces: Wetting, Patterning and Force Microscopy at Molecular Scale*. (eds. Ondarçuhu, T. & Aimé, J.P.) (Pan Stanford Publishing,) (2012).
47. Mingeot-Leclercq, M.-P., Deleu, M., Brasseur, R. & Dufrêne, Y.F. Atomic force microscopy of supported lipid bilayers. *Nat. Protoc.* **3**, 1654–1659 (2008).
48. D'Costa, N.P. & Hoh, J.H. Calibration of optical lever sensitivity for atomic force microscopy. *Rev. Sci. Instrum.* **66**, 5096–5097 (1995).